CHAPTER 1

Introduction

1.1. MOTIVATION FOR OPTICAL IMAGING

The most common medical imaging modalities include X-ray radiography, ultrasound imaging (ultrasonography), X-ray computed tomography (CT), and magnetic resonance imaging (MRI). The discovery of X rays in 1895, for which Roentgen received the first Nobel Prize in Physics in 1901, marked the advent of medical imaging. Ultrasonography, which is based on sonar, was introduced into medicine in the 1940s after World War II. The invention of CT in the 1970s, for which Cormack and Hounsfield received the Nobel Prize in Medicine in 1979, initiated digital cross-sectional imaging (tomography). The invention of MRI, also in the 1970s, for which Lauterbur and Mansfield received the Nobel Prize in Medicine in 2003, enabled functional imaging with high spatial resolution. Optical imaging, which is compared with the other modalities in Table 1.1, is currently emerging as a promising new addition to medical imaging.

Reasons for optical imaging of biological tissue include

1. Optical photons provide nonionizing and safe radiation for medical applications.
2. Optical spectra—based on absorption, fluorescence, or Raman scattering—provide biochemical information because they are related to molecular conformation.
3. Optical absorption, in particular, reveals angiogenesis and hypermetabolism, both of which are hallmarks of cancer; the former is related to the concentration of hemoglobin and the latter, to the oxygen saturation of hemoglobin. Therefore, optical absorption provides contrast for functional imaging.
4. Optical scattering spectra provide information about the size distribution of optical scatterers, such as cell nuclei.
5. Optical polarization provides information about structurally anisotropic tissue components, such as collagen and muscle fiber.

Biomedical Optics: Principles and Imaging, by Lihong V. Wang and Hsin-i Wu

TABLE 1.1. Comparison of Various Medical Imaging Modalities

Characteristics	X-ray Imaging	Ultrasonography	MRI	Optical Imaging
Soft-tissue contrast	Poor	Good	Excellent	Excellent
Spatial resolution	Excellent	Good	Good	Mixed[a]
Maximum imaging depth	Excellent	Good	Excellent	Good
Function	None	Good	Excellent	Excellent
Nonionizing radiation	No	Yes	Yes	Yes
Data acquisition	Fast	Fast	Slow	Fast
Cost	Low	Low	High	Low

[a]High in ballistic imaging (see Chapters 8–10) and photoacoustic tomography (see Chapter 12); low in diffuse optical tomography (see Chapter 11).

6. Optical frequency shifts due to the optical Doppler effect provide information about blood flow.
7. Optical properties of targeted contrast agents provide contrast for the molecular imaging of biomarkers.
8. Optical properties or bioluminescence of products from gene expression provide contrast for the molecular imaging of gene activities.
9. Optical spectroscopy permits simultaneous detection of multiple contrast agents.
10. Optical transparency in the eye provides a unique opportunity for high-resolution imaging of the retina.

1.2. GENERAL BEHAVIOR OF LIGHT IN BIOLOGICAL TISSUE

Most biological tissues are characterized by strong optical scattering and hence are referred to as either *scattering media* or *turbid media*. By contrast, optical absorption is weak in the 400–1350-nm spectral region. The mean free path between photon scattering events is on the order of 0.1 mm, whereas the mean absorption length (mean path length before photon absorption) can extend to 10–100 mm.

Photon propagation in biological tissue is illustrated in Figure 1.1. The light source is spatially a pencil beam (an infinitely narrow collimated beam) and temporally a Dirac delta pulse. The optical properties (see Appendix A) of the tissue include the following: refractive index $n = 1.37$, absorption coefficient $\mu_a = 1.4\ \text{cm}^{-1}$, scattering coefficient $\mu_s = 350\ \text{cm}^{-1}$, and scattering anisotropy $g = 0.8$. The mean free path equals 28 μm, corresponding to a propagation time of 0.13 ps. The transport mean free path equals 140 μm, corresponding to a propagation time of 0.64 ps. Note how widely the photons spread versus time in relation to the two time constants mentioned above. This diffusion-like behavior of light in biological tissue presents a key challenge for optical imaging. Various techniques have been designed to meet this challenge.

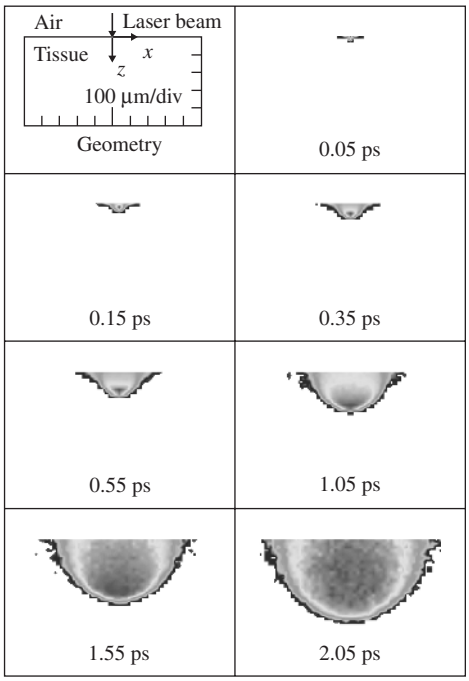

Figure 1.1. Snapshots of the simulated photon density distribution in a piece of biological tissue projected along the *y* axis, which points out of the paper.

1.3. BASIC PHYSICS OF LIGHT–MATTER INTERACTION

Absorption of a photon can elevate an electron of a molecule from the ground state to an excited state, which is termed *excitation*. Excitation can also be caused by other mechanisms, which are either mechanical (frictional) or chemical in nature. When an electron is raised to an excited state, there are several possible outcomes. The excited electron may relax to the ground state and give off luminescence (another photon) or heat. If another photon is produced, the emission process is referred to as *fluorescence* or *phosphorescence*, depending on the lifetime of the excited electron; otherwise, it is referred to as *nonradiative relaxation*. *Lifetime* is defined as the average time that an excited molecule spends in the excited state before returning to the ground state. The ratio of the number of photons emitted to the number of photons absorbed is referred to as the *quantum yield of fluorescence*. If the excited molecule is near another molecule with a similar electronic configuration, the energy may be transferred by excitation energy transfer—the excited electron in one molecule drops to the ground state while the energy is transferred to the neighboring molecule, raising an electron in that molecule to an excited state with a longer lifetime. Another possible outcome is photochemistry, in which an excited electron is actually transferred to another

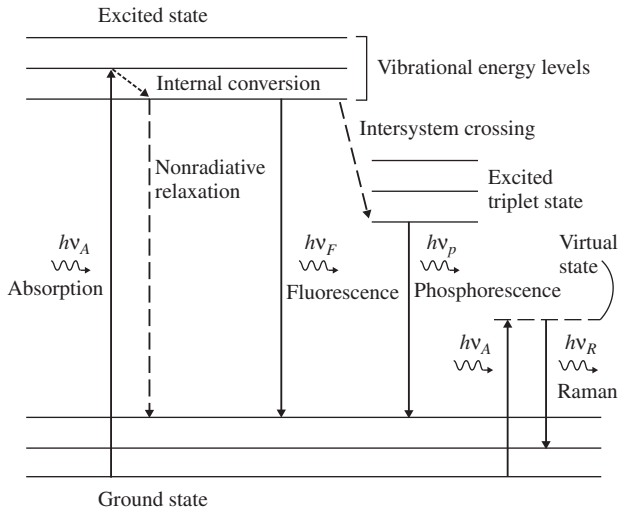

Figure 1.2. Jablonski energy diagram showing excitation and various possible relaxation mechanisms. Each $h\nu$ denotes the photon energy, where subscripts A, F, P, and R denote absorption, fluorescence, phosphorescence, and Raman scattering, respectively.

molecule. This type of electron transfer alters the chemical properties of both the electron donor and the electron acceptor, as in photosynthesis.

A Jablonski energy diagram describing electronic transitions between ground states and excited states is shown in Figure 1.2. Molecules can absorb photons that match the energy difference between two of their discrete energy levels, provided the transitions are allowed. These energy levels define the absorption and the emission bands.

Fluorescence involves three events with vastly different timescales. Excitation by a photon takes place in femtoseconds (1 fs $= 10^{-15}$ s, about one optical period). Vibrational relaxation (also referred to as *internal conversion*) of an excited-state electron to the lowest vibrational energy level in the excited state lasts for picoseconds (1 ps $= 10^{-12}$ s) and does not result in emission of a photon (nonradiative). Fluorescence emission lingers over nanoseconds (1 ns $= 10^{-9}$ s). Consequently, fluorescence lifetime is on the order of a nanosecond.

Phosphorescence is similar to fluorescence, but the excited molecule further transitions to a metastable state by intersystem crossing, which alters the electron spin. Because relaxation from the metastable state to the ground state is spin-forbidden, emission occurs only when thermal energy raises the electron to a state where relaxation is allowed. Consequently, phosphorescence depends on temperature and has a long lifetime (milliseconds or longer).

Two types of photon scattering by a molecule exist: elastic and inelastic (or Raman) scattering. The former involves no energy exchange between the photon and the molecule, whereas the latter does. Although both Raman scattering and fluorescence alter the optical wavelength, they have different mechanisms. In

Raman scattering, the molecule is excited to a virtual state; in fluorescence, the molecule is excited to a real stationary state. In both cases, the excited molecule relaxes to an energy level of the ground state and emits a photon. The molecule may either gain energy from, or lose energy to, the photon. If the molecule gains energy, the transition is known as a *Stokes transition*. Otherwise, the transition is known as an *anti-Stokes transition*. The scattered photon shifts its frequency accordingly since the total energy is conserved. Raman scattering can reveal the specific chemical composition and molecular structure of biological tissue, whereas elastic scattering can reveal the size distribution of the scatterers.

1.4. ABSORPTION AND ITS BIOLOGICAL ORIGINS

The *absorption coefficient* μ_a is defined as the probability of photon absorption in a medium per unit path length (strictly speaking, per unit infinitesimal path length). It has a representative value of 0.1 cm^{-1} in biological tissue. The reciprocal of μ_a is referred to as the *mean absorption length*.

For a single absorber, the absorption cross section σ_a, which indicates the absorbing capability, is related to its geometric cross-sectional area σ_g through the absorption efficiency $Q_a : \sigma_a = Q_a \sigma_g$. In a medium containing many absorbers with number density N_a, the absorption coefficient can be considered as the total cross-sectional area for absorption per unit volume:

$$\mu_a = N_a \sigma_a. \tag{1.1}$$

Here, absorption by different absorbers is considered to be independent.

According to the definition of the absorption coefficient, light attenuates as it propagates in an absorbing-only medium according to the following equation:

$$\frac{dI}{I} = -\mu_a \, dx, \tag{1.2}$$

where I denotes the light intensity and x denotes the distance along the light propagation direction. Equation (1.2) means that the percentage of light being absorbed in interval $(x, x + dx)$ is proportional to the product of μ_a and dx; the negative sign is due to the decrease of I as x increases. Integrating Eq. (1.2) leads to the well-known Beer law

$$I(x) = I_0 \exp(-\mu_a x), \tag{1.3}$$

where I_0 is the light intensity at $x = 0$. Beer's law actually holds even for a tortuous path. The transmittance is defined by

$$T(x) = \frac{I(x)}{I_0}, \tag{1.4}$$

which represents the probability of survival after propagation over x.

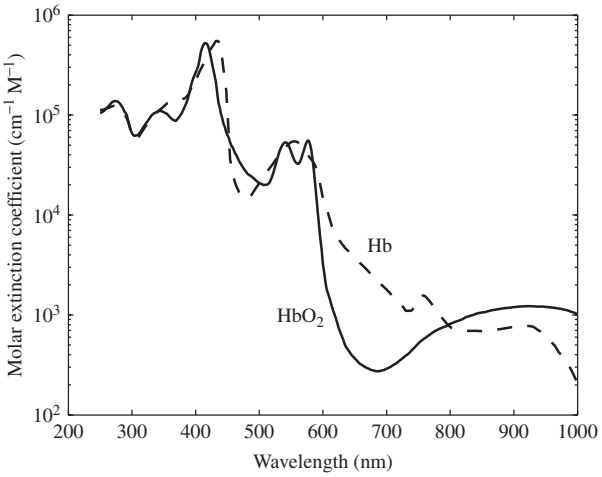

Figure 1.3. Molar extinction coefficients of oxy- and deoxyhemoglobin versus wavelength.

Optical absorption in biological tissue originates primarily from hemoglobin, melanin, and water. Hemoglobin has two forms: oxygenated and deoxygenated. Figure 1.3 shows the molar extinction coefficients—the extinction coefficient divided by ln(10) (see Section 7.3) per unit molar concentration—of oxy- and deoxyhemoglobin as a function of wavelength, where the extinction coefficient is defined as the probability of photon interaction with a medium per unit path length. Although extinction includes both absorption and scattering, absorption dominates scattering in hemoglobin. The molar extinction spectra of oxy- and deoxyhemoglobin are distinct but share a few intersections, termed *isosbestic points*. At these points, the absorption coefficient of an oxy- and deoxyhemoglobin mixture depends only on the total concentration, regardless of the oxygen saturation.

The absorption coefficients of some primary absorbing biological tissue components are plotted as a function of wavelength in Figure 1.4. Melanin absorbs ultraviolet (UV) light strongly but longer-wavelength light less strongly. Even water can be highly absorbing in some spectral regions. At the 2.95-μm water absorption peak, the penetration depth is less than 1 μm since $\mu_a = 12{,}694\ \text{cm}^{-1}$.

The absorption coefficients of biological tissue at two wavelengths can be used to estimate the concentrations of the two forms of hemoglobin based on the following equations:

$$\mu_a(\lambda_1) = \ln(10)\varepsilon_{\text{ox}}(\lambda_1)C_{\text{ox}} + \ln(10)\varepsilon_{\text{de}}(\lambda_1)C_{\text{de}}, \tag{1.5}$$

$$\mu_a(\lambda_2) = \ln(10)\varepsilon_{\text{ox}}(\lambda_2)C_{\text{ox}} + \ln(10)\varepsilon_{\text{de}}(\lambda_2)C_{\text{de}}. \tag{1.6}$$

Here, λ_1 and λ_2 are the two wavelengths; ε_{ox} and ε_{de} are the known molar extinction coefficients of oxy- and deoxyhemoglobin, respectively; C_{ox} and C_{de}

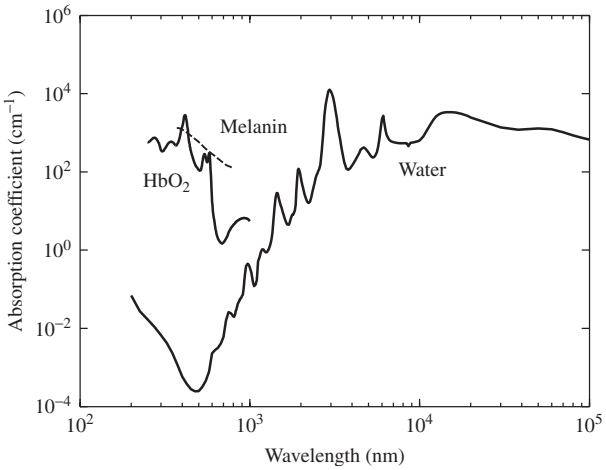

Figure 1.4. Absorption coefficients of primary biological absorbers.

are the molar concentrations of oxy- and deoxyhemoglobin, respectively, in the tissue. Once C_{ox} and C_{de} are obtained, the oxygen saturation (SO_2) and the total concentration (C_{Hb}) of hemoglobin can be computed as follows:

$$SO_2 = \frac{C_{ox}}{C_{ox} + C_{de}}, \tag{1.7}$$

$$C_{Hb} = C_{ox} + C_{de}. \tag{1.8}$$

This principle provides the basis for pulse oximetry and functional imaging. Angiogenesis can increase C_{Hb}, whereas tumor hypermetabolism can decrease SO_2.

1.5. SCATTERING AND ITS BIOLOGICAL ORIGINS

Scattering of light by a spherical particle of any size can be modeled exactly by the Mie theory, which reduces to the simpler Rayleigh theory if the spherical particle is much smaller than the wavelength. In a scattering medium containing many scatterers that are distributed randomly in space, photons usually encounter multiple scattering events. If scatterers are sparsely distributed (where the mean distance between particles is much greater than both the scatterer size and the wavelength), the medium is considered to be loosely packed. In this case, scattering events are considered to be independent; hence, single-scattering theory applies to each scattering event. Otherwise, the medium is considered to be densely packed. In this case, scattering events are coupled; thus, single-scattering theory does not apply. In this book, we consider only loosely packed scattering media. Keep in mind that one must differentiate a single coupled-scattering event (which involves multiple particles) from successive independent-scattering events (each of which involves a single particle).

The *scattering coefficient* μ_s is defined as the probability of photon scattering in a medium per unit path length. It has a representative value of 100 cm^{-1} in biological tissue. The reciprocal of μ_s is referred to as the *scattering mean free path*.

For a single scatterer, the scattering cross section σ_s, which indicates the scattering capability, is related to its geometric cross-sectional area σ_g through the scattering efficiency $Q_s : \sigma_s = Q_s \sigma_g$. For a medium containing many scatterers with number density N_s, the scattering coefficient can be considered as the total cross-sectional area for scattering per unit volume:

$$\mu_s = N_s \sigma_s. \tag{1.9}$$

The probability of no scattering (or ballistic transmittance T) after a photon propagates over path length x can be computed by Beer's law:

$$T(x) = \exp(-\mu_s x). \tag{1.10}$$

Optical scattering originates from light interaction with biological structures, which range from cell membranes to whole cells (Figure 1.5). Photons are scattered most strongly by a structure whose size matches the optical wavelength and whose refractive index mismatches that of the surrounding medium. The indices of refraction of common tissue components are 1.35–1.36 for extracellular fluid, 1.36–1.375 for cytoplasm, 1.38–1.41 for nuclei, 1.38–1.41 for mitochondria and organelles, and 1.6–1.7 for melanin. Cell nuclei and mitochondria are primary scatterers. The volume-averaged refractive index of most biological tissue falls within 1.34–1.62, which is greater than the refractive index of water (1.33).

The *extinction coefficient* μ_t, also referred to as the *total interaction coefficient*, is given by

$$\mu_t = \mu_a + \mu_s. \tag{1.11}$$

The reciprocal of μ_t is the mean free path between interaction events.

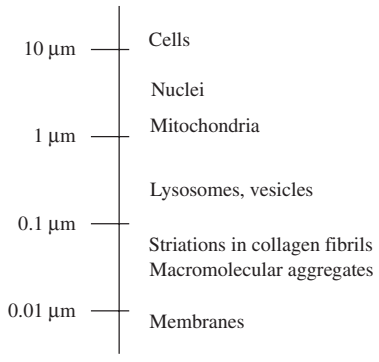

Figure 1.5. Biological structures of various sizes for photon scattering.

1.6. POLARIZATION AND ITS BIOLOGICAL ORIGINS

Linear birefringence (or simply birefringence), which is also known as *double refraction*, is the most important polarization property. A linearly birefringent material has dual principal indices of refraction associated with two linear polarization states of light (orientations of the electric field). The index of refraction for light polarization that is parallel with the optical axis of the material (e.g., the orientation of collagen fibers) is commonly denoted by n_e, while the light is referred to as the *extraordinary ray*. By contrast, the index of refraction for light polarization that is perpendicular to the optical axis is commonly denoted by n_o, while the light is referred to as the *ordinary ray*. If $n_e > n_o$, the birefringence is said to be positive. Conversely, if $n_e < n_o$, the birefringence is said to be negative.

Similarly, a circularly birefringent material has dual principal indices of refraction associated with the left and the right circular polarization states of light; as a result, it can rotate a linear polarization. The amount of rotation depends on the properties and the concentration of the active material, the optical wavelength, and the path length. If the other parameters are known, the amount of rotation can reveal the concentration.

Collagen, muscle fibers, myelin, retina, and keratin have linear birefringence. Collagen I is intensely positively birefringent, whereas collagen III is weakly negatively birefringent. Amino acids and glucose have circular birefringence; amino acids are levorotatory (exhibit left rotation) to linearly polarized light, whereas glucose is dextrorotatory (exhibits right rotation).

1.7. FLUORESCENCE AND ITS BIOLOGICAL ORIGINS

Fluorescence has the following characteristics:

1. Fluorescence light is red-shifted (wavelength is increased or frequency is reduced) relative to the excitation light; this phenomenon is known as the *Stokes shift*. The primary origins include the initial vibrational relaxations and the subsequent inclined fluorescence transitions to higher vibrational energy levels of the ground state. Other origins include excited-state reactions, complex formations, and resonance energy transfers.
2. Emission wavelengths are not only longer than but also independent of the excitation wavelength. Although the initial excited state is related to the excitation wavelength, a vibrational relaxation to the same intermediate state terminates the memory of such a relationship.
3. Fluorescence light is incoherent even if the excitation light is coherent because the uncertain delays in the vibrational relaxations spread over more than one light period.
4. Fluorescence spectrum, when plotted against the frequency, is generally a mirror image of the absorption spectrum for the following reasons: (a) before excitation, almost all the molecules are at the lowest vibrational energy level of the ground state; (b) before emission, almost all the

molecules are at the lowest vibrational energy level of the first excited state; (c) the least photon energy for excitation equals the greatest emission photon energy; (d) the vibrational energy levels in the ground and first excited states have similar spacing structures; and (e) the probability of a ground-state electron excited to a particular vibrational energy level in the first excited state is similar to that of an excited electron returning to a corresponding vibrational energy level in the ground state.

The properties of some endogenous fluorophores are listed in Table 1.2 (where λ_a denotes maximum absorption wavelength; ε denotes molar extinction coefficient; λ_x denotes maximum excitation wavelength; λ_m denotes maximum emission wavelength; Y denotes quantum yield of fluorescence). Fluorescence can provide information about the structure, dynamics, and interaction of a bioassembly. For example, mitochondrial fluorophore NADH (nicotinamide adenine dinucleotide, reduced form) is a key discriminator in cancer detection; it tends to be more abundant in cancer cells owing to their higher metabolic rate. NAD(P)H (nicotinamide adenine dinucleotide phosphate, reduced form) has a lifetime of 0.4 ns when free but a longer lifetime of 1–3 ns when bound.

1.8. IMAGE CHARACTERIZATION

Several parameters are important in the characterization of medical images. In this section, the discussion is limited primarily to two-dimensional (2D) images, but the principles involved can be extended to one-dimensional (1D) or three-dimensional (3D) images.

When a high-contrast point target is imaged, the point appears as a blurred blob in the image because any practical imaging system is imperfect. The spatial distribution of this blob in the image is referred to as the *point spread function* (PSF). The PSF is sometimes called the *impulse response* (or Green's function) because

TABLE 1.2. Properties of Endogenous Fluorophores at Physiologic pH

Fluorophore	λ_a (nm)	ε ($cm^{-1}M^{-1}$)	λ_x (nm)	λ_m (nm)	Y
Ceroid	—	—	340–395	430–460 540–640	—
Collagen, elastin	—	—	325	400	—
FAD	—	—	450	515	—
Lipofuscin	—	—	340–395	430–460 540–540	—
NAD^+	260	18×10^3	—	—	—
NADH	260	14.4×10^3	290	440	—
	340	6.2×10^3	340	450	—
Phenylalanine	260	0.2×10^3	—	280	0.04
Tryptophan	280	5.6×10^3	280	350	0.2
Tyrosine	275	1.4×10^3	—	300	0.1

a geometric point can be represented by a spatial Dirac delta function (an impulse function). When two point targets are too close to each other, the combined blob in the image can no longer be clearly resolved into two entities. The full width at half maximum (FWHM) of the PSF is often defined as the spatial resolution. Even though an ideal geometric point target cannot be constructed or detected in reality, a point target needs only to be much smaller than the spatial resolution.

Sometimes, a line spread function (LSF), which is the system response to a high-contrast geometric line, is measured instead of a PSF. For a linear system, an LSF can be related to a PSF on the (x, y) plane by

$$\mathrm{LSF}(x) = \int \mathrm{PSF}(x, y)\, dy. \tag{1.12}$$

Likewise, an edge spread function (ESF), which is the system response to a high-contrast semiinfinite straight edge, can be measured as well. For a linear system, an ESF can be related to an LSF as follows (Figure 1.6):

$$\mathrm{ESF}(x) = \int_{-\infty}^{x} \mathrm{LSF}(x')\, dx', \tag{1.13}$$

$$\mathrm{LSF}(x) = \frac{d}{dx}\mathrm{ESF}(x). \tag{1.14}$$

In a linear, stationary, and spatially translation-invariant system, image function $i(\vec{r})$ equals the convolution of object function $o(\vec{r})$ with point spread function $\mathrm{PSF}(\vec{r})$:

$$i(\vec{r}) = o(\vec{r}) * * \mathrm{PSF}(\vec{r}), \tag{1.15}$$

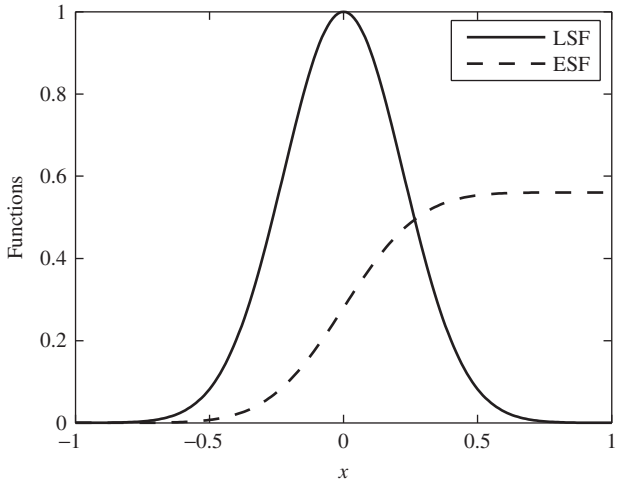

Figure 1.6. Illustration of an LSF and an ESF.

where $\vec{r} = (x, y)$ and $**$ represents 2D spatial convolution. Equation (1.15) can be expressed in several forms:

$$\begin{aligned} i(\vec{r}) &= \iint o(\vec{r}')\mathrm{PSF}(\vec{r} - \vec{r}')\, d\vec{r}' \\ &= \iint o(x', y')\mathrm{PSF}(x - x', y - y')\, dx'\, dy' \\ &= \iint o(\vec{r} - \vec{r}'')\mathrm{PSF}(\vec{r}'')\, d\vec{r}''. \end{aligned} \tag{1.16}$$

Taking the 2D Fourier transformation of Eq. (1.15) yields

$$I(\rho, \xi) = O(\rho, \xi)H(\rho, \xi). \tag{1.17}$$

Here, ρ and ξ represent the spatial frequencies; I represents the image spectrum; O represents the object spectrum; and H represents the PSF spectrum, which is the system transfer function (STF). The amplitude of the STF is referred to as the *modulation transfer function* (MTF):

$$\mathrm{MTF}(\rho, \xi) = |H(\rho, \xi)|. \tag{1.18}$$

Similarly, for an LSF, the MTF is based on the 1D Fourier transformation:

$$\mathrm{MTF}(\rho) = \left| \int_{-\infty}^{+\infty} \exp(-j2\pi\rho x)[\mathrm{LSF}(x)]\, dx \right|. \tag{1.19}$$

Most imaging systems act as lowpass filters, resulting in blurring of the fine structures.

The visibility of a structure in an image depends on, among other factors, the contrast C:

$$C = \frac{\Delta I}{\langle I \rangle}. \tag{1.20}$$

While $\langle I \rangle$ is the average background image intensity, ΔI is the intensity variation in the region of interest (Figure 1.7).

Contrast does not represent a fundamental limitation on visualization since it can be artificially enhanced by, for example, subtracting part of the background (thresholding) or raising the intensity to some power. Statistical noise does, however, represent a fundamental limitation. The signal-to-noise ratio (SNR) is defined as

$$\mathrm{SNR} = \frac{\langle I \rangle}{\sigma_I}, \tag{1.21}$$

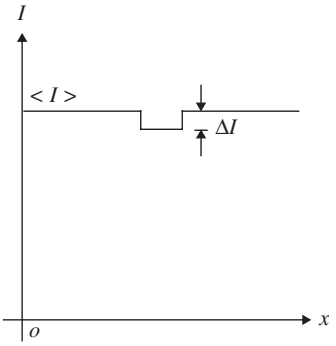

Figure 1.7. Illustration of image contrast.

where σ_I denotes the standard deviation of the background intensity, that is, the noise representing the root-mean-squared (rms) value of the intensity fluctuations.

Ultimately, the ability to visualize a structure depends on the contrast-to-noise ratio (CNR), which is defined as

$$\text{CNR} = \frac{\Delta I}{\sigma_I}, \tag{1.22}$$

which can be rewritten as

$$\text{CNR} = C \cdot \text{SNR}. \tag{1.23}$$

The *field of view* (FOV) in an image refers to the extent of the image field that can be seen all at once. A tradeoff often exists between FOV and spatial resolution. For example, "zooming in" with a camera compromises the FOV for resolution.

The maximum imaging depth in tomography is the depth limit at which the SNR or the CNR is acceptable. A tradeoff often exists between maximum imaging depth and depth resolution. The ratio of maximum imaging depth to depth resolution, referred to as the *depth-to-resolution ratio* (DRR), represents the number of effective pixels in the depth dimension. A DRR of 100 or greater is considered to indicate high resolution in terms of pixel count.

The *frame rate* is defined as the number of frames of an animation that are displayed per second, measured in frames per second (fps); it measures how rapidly an imaging system produces consecutive 2D images. At or above the video rate (30 fps), the human eye cannot resolve the transition of images; hence, the animation appears smooth.

In this book, the object to be imaged is typically a scattering medium, which can be a biological tissue phantom, a sample (specimen) of biological tissue, or an insitu or invivo biological entity. Sometimes, "sample" refers broadly to the object to be imaged.

Example 1.1. Derive Eq. (1.13).

On the basis of 1D convolution followed by a change of variable, we derive

$$\begin{aligned}\mathrm{ESF}(x) &= \int_0^{+\infty} \mathrm{LSF}(x - x')\, dx' = \int_x^{-\infty} \mathrm{LSF}(x'')\, d(-x'') \\ &= \int_{-\infty}^{x} \mathrm{LSF}(x')\, dx'. \end{aligned} \tag{1.24}$$

PROBLEMS

1.1 Derive the following relationship between electromagnetic wavelength λ in the unit of μm and photon energy $h\nu$ in electron volts (eV): $\lambda h\nu = 1.24$, where h denotes the Planck constant and ν denotes the electromagnetic frequency.

1.2 In a purely absorbing (nonscattering) medium with absorption coefficient μ_a, what percentage of light is left after a lightbeam propagates a length of L? Plot this percentage as a function of L in MATLAB.

1.3 In a purely absorbing (nonscattering) medium with absorption coefficient μ_a, derive the average length of survival of a photon.

1.4 In a purely scattering (nonabsorbing) medium with scattering coefficient μ_s, what percentage of light has not been scattered after the original lightbeam propagates a length of L?

1.5 In a purely scattering (nonabsorbing) medium with scattering coefficient μ_s, derive the average length of survival of a photon.

1.6 In a scattering medium with absorption coefficient μ_a and scattering coefficient μ_s, what percentage of light has survived scattering and absorption after the original lightbeam propagates a length of L? Of the percentage that has been absorbed and scattered, what is the percentage that has been absorbed?

1.7 In MATLAB, draw a 2D diagram to simulate a random walk by following the subsequent steps: (1) start the point at (0,0); (2) sample a random number x_1 that is evenly distributed in interval (0,1]; (3) determine a step size by $s = 100 \ln(x_1)$; (2) sample a random number x_2 that is evenly distributed in interval (0,1]; (4) determine an angle by $\alpha = 2\pi x_2$; (5) move the point by step size s along angle α; (6) repeat steps 2–5 20 times to obtain a trajectory; (7) repeat steps 1–6 3 times to trace multiple trajectories.

1.8 Derive the oxygen saturation SO_2 and the total concentration of hemoglobin C_{Hb} based on Eqs. (1.5) and (1.6).

1.9 Download the data for the molar extinction coefficients of oxy- and deoxy-hemoglobin as a function of wavelength from the Web (URL: http://omlc.ogi.edu/spectra/) and plot the two curves in MATLAB.

1.10 Download the data for the molar extinction coefficients of oxy- and deoxy-hemoglobin as a function of wavelength from the Web (URL: http://omlc.ogi.edu/spectra/). Download the data for the absorption coefficient of pure water as a function of wavelength as well. Using physiologically representative values for both oxygen saturation SO_2 and total concentration of hemoglobin C_{Hb}, compute the corresponding absorption coefficients. Plot the three absorption spectra on the same plot in MATLAB. Identify the low-absorption near-IR window that provides deep penetration.

READING

Drezek R, Dunn A, and Richards-Kortum R (1999): Light scattering from cells: Finite-difference time-domain simulations and goniometric measurements, *Appl. Opt.* **38**: 3651–3661. [See Section 1.5, above (in this book).]

Jacques SL (2005): From http://omlc.ogi.edu/spectra/ and http://omlc.ogi.edu/classroom/. (See Sections 1.5 and 1.6, above.)

Richards-Kortum R and Sevick-Muraca E (1996): Quantitative optical spectroscopy for tissue diagnosis, *Ann. Rev. Phys. Chem.* **47**: 555–606. (See Section 1.7, above.)

Wang LHV and Jacques SL (1994): Animated simulation of light transport in tissues. Laser-tissue interaction V, *SPIE* 2134: 247–254. (See Section 1.2, above.)

Wang LHV, Jacques SL, and Zheng LQ (1995): MCML—Monte Carlo modeling of photon transport in multi-layered tissues, *Comput. Meth. Prog. Biomed.* **47**(2): 131–146. (See Section 1.2, above.)

Wang LHV (2003): Ultrasound-mediated biophotonic imaging: A review of acousto-optical tomography and photo-acoustic tomography, *Disease Markers* **19**(2–3): 123–138. (See Section 1.1, above.)

FURTHER READING

Hecht E (2002): *Optics*, Addison-Wesley, Reading, MA.

Lakowicz JR (1999): *Principles of Fluorescence Spectroscopy*, Kluwer Academic/Plenum, New York.

Macovski A (1983): *Medical Imaging Systems*, Prentice-Hall, Englewood Cliffs, NJ.

Mourant JR, Freyer JP, Hielscher AH, Eick AA, Shen D, and Johnson TM (1998): Mechanisms of light scattering from biological cells relevant to noninvasive optical-tissue diagnostics, *Appl Opt.* **37**(16): 3586–3593.

Shung KK, Smith MB, and Tsui BMW (1992): *Principles of Medical Imaging*, Academic Press, San Diego.

Tuchin VV (2000): *Tissue Optics: Light Scattering Methods and Instruments for Medical Diagnosis*, SPIE Optical Engineering Press, Bellingham, WA.

Welch AJ and van Gemert MJC (1995): *Optical-Thermal Response of Laser-Irradiated Tissue*, Plenum Press, New York.